Central Retina Functional Damage in Usher Syndrome Type 2: 22 Years of Focal Macular ERG Analysis in a Patient Population From Central and Southern Italy

Lucia Galli-Resta,[1] Giorgio Placidi,[2] Francesca Campagna,[2] Lucia Ziccardi,[3] Marco Piccardi,[2] Angelo Minnella,[2] Edoardo Abed,[2] Silvia Iovine,[2] Paolo Maltese,[4] Matteo Bertelli,[4] and Benedetto Falsini[2]

[1]Istituto di Neuroscienze CNR, Pisa, Italy
[2]Department of Ophthalmology, Policlinico Gemelli, Università Cattolica del Sacro Cuore, Rome, Italy
[3]Fondazione Bietti, IRCSS, Rome, Italy
[4]Medical Genetics Laboratory, MAGI Euregio SCS, Bolzano, Italy

Correspondence: Benedetto Falsini, Istituto di Oftalmologia, Policlinico Gemelli, Università Cattolica del Sacro Cuore, Largo Agostino Gemelli, 8, Rome 00168, Italy; benedetto.falsini@unicatt.it.

Submitted: December 21, 2017
Accepted: June 10, 2018

Citation: Galli-Resta L, Placidi G, Campagna F, et al. Central retina functional damage in Usher syndrome type 2: 22 years of focal macular ERG analysis in a patient population from central and southern Italy. *Invest Ophthalmol Vis Sci*. 2018;59:3827–3835. https://doi.org/10.1167/iovs.17-23703

Purpose. Recent studies show that patients with Usher syndrome type 2 (USH2) have abnormal cone structure and density in the central retina. This occurs in the presence of normal acuity, opening the quest for additional sensitive functional measures of central cone function in USH. We tested here whether focal macular cone electroretinogram (fERG) could be such a tool.

Methods. This retrospective study of central cone function loss was based on data from 47 patients with USH2 from the Ophthalmology Department of the Policlinico Gemelli/Catholic University in Rome. The analysis focused on the decrease of the fERG, obtained in response to a 41-Hz sinusoidal modulation of a uniform field presented to the central 18°, generated by red light-emitting diodes (LEDs) and superimposed on an equiluminant steady adapting background. fERG decrease was compared with the decrease of best-corrected visual acuity and Goldmann kinetic perimetry V4E field.

Results. fERG follow-up data document a severe and precocious loss of central cone function in USH2 patients, preceding losses in other measures of cone function. fERG is already reduced to 40% of control at the beginning of the second decade of life, and by 25 years of age, all USH2 patients have fERGs less than 30% of control values.

Conclusions. fERG represents a sensitive tool to evaluate central cone function in USH2, anticipating the decline of other central cone function measures, such as visual acuity and Goldmann perimetry.

Keywords: retinitis pigmentosa, cone photoreceptors, retina, Goldmann perimetry

Usher syndrome (USH) is an autosomal recessive group of diseases characterized by the association of retinitis pigmentosa (RP)-like retinal degeneration with bilateral sensory-neural hearing loss.[1] On the basis of clinical studies[2] and genetic surveys,[3–5] the prevalence of USH is estimated to be between 1/10,000 and 1/50,000 people.

USH is the most common cause of deaf-blindness,[6] and the most frequent form of recessive RP, comprising 18% of all RPs.[7] Three clinical subtypes are distinguishable, on the basis of the degree and onset of hearing loss, the presence or absence of vestibular abnormality, and the age of RP onset.[8,9]

Usher type 2 (USH2) is the most common of the three USH subtypes, comprising 56% to 75% of USH patients.[10–13] USH2 is characterized by the lack of vestibular deficits and mild to generally moderate degrees of congenital neurosensory hearing loss; and, RP onset is usually in the second decade of life.[9] In USH2 patients, RP symptoms typically start with a concentric visual field loss, whereas visual acuity remains well preserved for a long time.[14,15] Indeed, progression of visual field loss may occur at a much faster rate than losses in visual acuity or cone-mediated central light-adapted perimetry.[14–16]

Visual field testing, visual acuity, and central perimetry do not directly assess retinal abnormalities, but rather global visual performance, as the subject is required to respond to the perceived stimuli. The use of objective tests specific for retinal functions, such as foveal densitometry,[17] multifocal electroretinogram (ERG),[18] and focal macular ERGs (fERGs),[19] shows early central cone functional abnormalities in USH patients, as some psychophysical studies do, showing early abnormal foveal spectral sensitivity to short-wavelength light.[20] Indeed, USH patients may complain of central visual problems from the early stages, reporting the need for high contrast visual stimuli for better central vision, such as the need to shine a strong light on the interlocutor's lips to allow speech-reading (Falsini, unpublished).

Thus, although the concept of a peripheral to central progression of the visual symptoms in USH disease is deeply rooted, and likely corresponds to the relative severity of the symptoms as perceived by patients, a more complex picture of disease progression is very likely.

Anatomic studies also provide a complex picture of RP in USH syndrome. Optical coherence tomography (OCT) in the early stages of USH1 visual disease show the presence of a transition zone between the relatively preserved central retina and the more affected periphery.[21] Typically, the ellipsoid zone band in the central macular area of patients with USH1 is reduced in extent only at the late stages of the disease, with an accompanying loss of the outer nuclear layer, and profound losses in light-adapted, cone-mediated sensitivity in the central and paracentral retinal regions. In USH2 however, abnormal sensitivity has also been reported within the central region encompassed by the intact ellipsoid zone in the early disease stages.[22] Confocal and nonconfocal split-detector adaptive optics scanning light ophthalmoscopy (AOSLO) shows that central and paracentral cones in USH may be altered in their structure and probably in their waveguide function long before visual acuity loss. Furthermore, it indicates that the number of cones is significantly reduced in the central retina of patients with USH, compared with control values.[22]

Taken together, these studies suggest that alongside severe peripheral deficits, loss of both structure and function of the central cone system in USH may characterize the early stages of the disease, preceding losses in visual acuity and perimetric sensitivity. Thus, identifying other sensitive functional measures of central retina cone function may certainly be helpful.

In the last 22 years, in the routine testing USH patients, we have used a fast and noninvasive measure of central cone function, the fERG. The fERG is obtained in response to the 41-Hz sinusoidal modulation of a uniform field presented to the central 18°, generated by red light-emitting diodes (LEDs) and superimposed on an equiluminant steady adapting background. The fERG first harmonic correlates with perimetric sensitivity in the same retinal region.[19] In previous studies, we used fERG to estimate the rate of central cone function decay in different subtypes of RP,[23] and in patients with cone dystrophy.[24,25]

Here, in a retrospective study, we present the evaluation of central cone function by f ERG in a cohort of 47 patients with USH2. Rather than focusing on the relative decay rate, as we did in the past,[23] we evaluated the absolute values of fERG measures and their decrease with age, comparing such decrease with changes in visual acuity and Goldmann kinetic perimetry V4e. The results show that fERG documents a severe and precocious loss of central cone function in patients with USH2, anticipating losses in other measures of cone function.

Methods

Patients

Forty-seven subjects (aged 12–75 years) affected by USH2 were included in the study. Patients were clinically followed at the Institute of Ophthalmology, Visual Electrophysiology Service at Fondazione Policlinico Gemelli/Università Cattolica del S. Cuore. With one exception, all patients were from central and southern Italy (Supplementary Fig. S1).

A detailed medical and family history was obtained from the patient and/or their parents. This included information regarding age of diagnosis of hearing loss, nature of hearing loss, age of perceived night blindness, age of RP diagnosis as well as information regarding motor development (age at which the patient first sat and walked, as well as whether and when the patient learned to use a bicycle, a discriminating criterion for vestibular integrity).

The diagnosis of USH2 was based on the lack of vestibular deficits, the presence of a mild to generally moderate degree of congenital neurosensory hearing loss, and RP. Audiometric evaluations were available for most patients and showed bilateral sensory hearing loss with a down-sloping configuration.[26] RP was diagnosed on the basis of a history of night-blindness, typical retinal pigmentary changes, subnormal or undetectable full-field electroretinographic amplitudes, and progressive peripheral visual field loss.

Patients had a known inheritance pattern, and 23 of 47 patients also had identified genetic USH2a variants. Exclusion criteria were the presence of severe ocular media opacities, or concomitant ocular (e.g., glaucoma, amblyopia) or systemic diseases. The demographic data for individual patients are reported in Table 1. Table 2 provides the variant details for the 23 patients with identified genetic variants.

Informed consent to participate in the study was obtained from all patients and control subjects, or their parents, after the aims and modalities of the investigation had been fully explained. The study followed the tenets of the Declaration of Helsinki and was approved by the Ethics Committee of the institution.

Table 1. Demographic Data of the USH2 Cohort Analyzed

Pt Number	Sex	Age, First Visit	Follow-Up, y	*N* Visits
1	f	27	4	4
2	f	20		1
3	m	50	10	7
4	f	35		1
5	m	29	2	3
6	m	12	9	7
7	f	33		1
8	m	42		1
9	f	69		1
10	f	59	2	3
11	m	21	5	4
12	f	58	1	2
13	m	43		1
14	f	55	1	2
15	f	49	1	2
16	m	33		1
17	m	18	5	6
18	f	31	2	3
19	m	14		1
20	m	48	1	2
21*	f	53	22	18
22	f	21		1
23	f	27		1
24	f	53		1
25	m	21		1
26	m	32	14	6
27	f	69	5	3
28	f	24	7	3
29	m	17	8	8
30	f	51	9	10
31	m	23	16	14
32†	f	47	5	4
33†	m	37	7	4
34	m	29	2	3
35	m	39	1	2
36‡	f	14	5	3
37‡	m	22	22	14
38	f	32	5	4
39	f	48		1
40	m	15	18	13
41	m	56	2	2
42*	m	60	4	5
43	f	36		1
44	m	37		1
45	m	62	3	4
46	f	45	13	8
47	f	55	8	7

f, female; m, male; Pt, patient.
* Sibling pairs.
† Sibling pairs.
‡ Sibling pairs.

Table 2. Patient Subset With Identified Genetic Variants

			uSH2A Variants (NM_206933.2)				
Pt Number	Sex	Allele State	Nucleotide Change	Amino Acid Change	refSNP	MAF	Variant Interpretation †
8	M	hom	c.908G>A	p.(Arg303His)	rs371777049	T=0.00005/6 (ExAC)	**Pathogenic**
9	F	het	c.2299del	p.(Glu767serfs*21)			Pathogenic
		het	c.4046del	p.(ser1349Phefs*17)			Pathogenic
10	F	hom	c.2810 2993del	p.(Gly937Aspfs*13)			Pathogenic
12	F	hom	c.9815C>T	p.(Pro3272Leu)		A=3.308e-05/4 (ExAC)	Likely Pathogenic
13	M	het	c.7068T>G	p.(Asn2356Lys)	rs200038092	C=0.0008/95 (ExAC)	**vuS**
		het	c.14091del	p.(Phe4697fs)			Pathogenic
14	F	het	c.2209C>T	p.(Arg737*)	rs111033334	A=0.000008/1 (ExAC)	**Pathogenic**
		het	c.13447G>C	p.(Gly4483Arg)		G=8.245e-06 /1 (ExAC)	vus
	M	het	c.15199del	p.(lle5067serfs*23)			Pathogenic
19		het	c.10712C>T	p.(Thr3571Met)	rs202175091	A=0.00002/2 (ExAC)	**Likely Pathogenic**
20	M	het	c.990 991del	p.(Asn330Lysfs*8)			Pathogenic
		het	c.10712C>T	p.(Thr3571Met)	rs202175091	A=0.00002/2 (ExAC)	**Likely Pathogenic**
21	F	het	c.2276G>T	p.(Cys759Phe)	rs80338902	A=0.0008/95 (ExAC)	**Pathogenic**
		het	c.3215T>G	p.(Leu1072Arg)			vus
22	F	het	c.13130C>A	p.(ser4377*)	rs111033385	T=0.000008/1 (ExAC)	**Pathogenic**
		het	c.653T>A	p.(val218Glu)	rs397518026	T=0.00004/5 (ExAC)	**Likely Pathogenic**
23	F	hom	c.9815C>T	p.(Pro3272Leu)		A=3.308e-05/4 (ExAC)	Likely Pathogenic
25	M	hom	c.14248C>T	p.(Gln4750*)	rs727504867		**Pathogenic**
26	M	het	c.802G>A	p.(Gly268Arg)	rs111033280	T=0.000008/1 (ExAC)	**vuS**
		het	c.10437G>T	p.(Trp3479Cys)			vus
28	F	het	c.(1644+1 1645-1)(2293+1 2294-1)dup				Pathogenic
		het	c.12067-2A>G		rs397517978	C=0.00007/8 (ExAC)	Pathogenic
31	M	het	c.8584C>T	p.(Gln2862*)			Pathogenic
		het	c.13018G>C	p.(Gly4340Arg)			vus
34	M	hom	c.10699del	p.(Leu3567*)			Pathogenic
35	M	het	c.5959T>A	p.(Tyr1987Asn)	rs747652397	T=0.00002/3 (ExAC)	vus
		het	c.10451G>A	p.(Arg3484Gln)	rs771999994	T=0.00008/10 (ExAC)	vus
37	M	het	c.2299del	p.(Glu767serfs*21)	rs80338903	del G=0.0008/96 (ExAC)	**Pathogenic**
		het	c.4714C>T	p.(Leu1572Phe)	rs111033333	A=0.0008/95 (ExAC)	**Likely Benign**
40	M	hom	c.12006C>A	p.(Tyr4002*)			Pathogenic
	M	het	c.2276G>T	p.(Cys759Phe)	rs80338902	A=0.0008/95 (ExAC)	**Pathogenic**
41		het	c.14286C>A	p.(Asn4762Lys)	rs750368946	A=0.00002/2 (ExAC)	vus
43	F	het	c.1055C>T	p.(Thr352lle)			Likely Pathogenic
		het	c.10712C>T	p.(Thr3571Met)	rs202175091	A=0.00002/2 (ExAC)	**Likely Pathogenic**
44	M	het	c.12381 12382del	p.(Tyr4128Hisfs*24)			Pathogenic
		het	c.2299del	p.(Glu767serfs*21)			Pathogenic
46	F	hom	c.5221T>C	p.(ser1741Pro)			vus

Bold indicates ClinVar last evaluation; normal, classified in this study according to the criteria by the American College of Medical Genetics and Genomics Standards and Guidelines.[44] Het, heterozygous; Hom, homozygous; MAF, minor allele frequency; VuS, variant of uncertain significance.

Molecular Genetic Analysis

In-solution target enrichment ("Nextera Rapid Capture Enrichment") on the Illumina platform (Illumina, San Diego, CA, USA) was performed to sequence all coding exons and flanking exon/intron boundaries of the genes known to be associated with USH2.[27] The raw read data, in fastq format, were analyzed to generate the list of sequence variants using an in-house pipeline, as previously described.[28]

Measures of Ocular Function and Electroretinography

For each patient, a full, general, and ophthalmologic examination (including detailed family history, anterior segment biomicroscopy, corrected visual acuity, direct and indirect ophthalmoscopy, IOP measurement, and flash ERGs recorded according to International Society for Clinical Electrophysiology of Vision [ISCEV] standard protocols) was performed at baseline. Best-corrected visual acuity (BCVA) was obtained with a standardized, projected Snellen chart. Kinetic visual fields were measured for the V4e white test light of the Goldmann perimeter against the standard background of 31.5 apostilbs.

Cone-mediated fERG was recorded from the central 18° region using a uniform red field stimulus superimposed on an equiluminant steady adapting background, used to minimize stray-light modulation. The stimulus was generated by a circular array of eight red LEDs (k maximum 660 nm, mean luminance 93 cd/m^2) presented on the rear of a Ganzfeld bowl (white-adapting background, luminance: 40 cd/m^2). A diffusing filter in front of the LED array made it appear as a circle of uniform red light. fERGs were recorded in response to the sinusoidal 95% luminance modulation of the central red field. The flickering frequency was 41 Hz. This apparatus has been the same throughout the years, with periodic controls of LED and background intensity. Patients fixated monocularly at a 0.25° central fixation mark, under the constant monitoring of an external observer. Pupils were pharmacologically (1% tropicamide and 2.5% phenylephrine hydrochloride) dilated to a diameter of 8 mm, and all subjects underwent a preadaptation period of 20 minutes to the stimulus mean illuminance. fERGs were recorded by an Ag-AgCl electrode taped on the skin over the lower eyelid. A similar electrode, placed over the eyelid of the contralateral-patched eye, was used as reference (interocular recording). fERG signals were amplified (100,000-fold), bandpass filtered between 1 and 100 Hz (6 decibels/octave [dB/oct]), and averaged (12-bit resolution, 2-kHz sampling rate, 200–600 repetitions in 2–6 blocks). Off-line discrete Fourier analysis quantified the peak-to-peak amplitude and phase lag of the response fundamental harmonic (first harmonic) at 41 Hz.

Data Acquisition and Analysis

For each patient, fERG measurements were obtained for each eye, with the routine testing sequence of right eye–left eye–left eye–right eye. The fERG value for each eye was the average of its two recordings. For each patient, we determined the eye with better fERG at the first visit and followed the results for this eye for all the measurements we analyzed.

To minimize nonnormality, quantitative analyses used the logMAR for visual acuity fractions,[29] and the first harmonic peak-to-peak amplitude as a measure of the fERG amplitude.[30]

All data analysis and plots were made using OriginPro 2015 (OriginLab Corporation, Northampton, MA, USA).

Goldmann Area Measure. Kinetic Goldmann visual field maps were scanned as high-resolution TIFF images. These images where then analyzed with Metamorph Offline (ver 5.0; Universal Imaging Corp., West Chester, PA, USA), a quantitative image analysis software. Briefly, for each field, the length of the 90° to 90° horizontal axis and the 70° to 70° vertical axis were measured with the line tool for calibration. The Goldmann V4e field map was then traced with the area tool to obtain its area in pixels. This was then converted into degrees squared using the calibration obtained with the horizontal and vertical axis measurements. Area values were entered into a log file together with patient and time data. The V4e isopter was selected because it was available for all the patients and has been used in many previous studies.[14–16,31]

Cross-Sectional Time-Course Curves. Cross-sectional time-course curves were obtained by assigning each patient data to the appropriate age bin (selected binning covered the 10- to 70-year span, with a 5-year bin size for fERG and a 10-year bin size for BCVA and Goldmann V4e). For patients with more than one measure within an age bin, the average value for the bin was computed, so that each patient contributed only one value to each age bin. The mean value, SD, and number of contributing patients were then computed for each age bin. The same procedure was followed to obtain the cross-sectional time-course curve for fERG for control subjects.

The mean logMAR for control subjects was by definition 0 (corresponding to a 20/20 BCVA), with 0 SD. Data for control Goldmann V4e were derived from 20 eyes of 10 age-matched healthy subjects. The range of these control data is in agreement with previous studies.[14,15]

The small number of control subjects for age group prevented us from estimating the time course of the fifth percentile with age. However, considering that fERG in control subjects decreased 25% over the entire age span analyzed, we estimated an average fifth percentile of fERG in control subjects by pooling together all data, irrespective of age.

Estimated Average Annual Rate of Decline for fERG. The average annual rate of decline for fERG within the 10 to 25 years age range was estimated by fitting the cross-sectional fERG curve with an exponential decline, as in previous studies.[29]

Plot of USH2 Data as Percentage of Control Data. To plot USH2 patient data as percentage of healthy control data, we expressed the cross-sectional mean and SD as percentages of the control subject average value. In the case of fERG and Goldmann V4e area, the range between 0 and the mean value for control subjects was considered to be 0% to 100% percentage range (100% = control mean value, 0% = 0). In the case of logMAR, a logMAR equal to 0 (BCVA = 20/20 decimal) was considered = 100% of normal control, and a logMAR of 2 (BCVA = 2/200 decimal) was considered = 0%.

Statistical Analysis

Data are presented as mean ± SD, unless otherwise specified. Statistical analysis was performed using Prism 6.0 (GraphPad Software, Inc., La Jolla, CA, USA).

Results

This retrospective study is based on data from 47 patients with a clinical diagnosis of USH2. All patients were clinically followed at the Ophthalmology Department of the Catholic University in Rome. The cohort comprised 24 females and 23 males. Mean age at first visit was 37.6 years (SD 15.5, minimum 12, maximum 69, oldest at the last visit, 75 years).

For 15 patients, only fERG recordings from one visit (first visit) were available. The remaining 32 patients (17 males, 15 females; average age at first visit 38.8 years, SD 16.6, median 38, minimum 12, maximum 69 years) had an average fERG follow-up of 6.8 years (SD 6.0, median 5, minimum 1 maximum 22 years, see Table 1). Data were acquired in 253 visits, spanning the years 1995 to 2017.

fERG Amplitude Versus Age

Typical fERG recordings from a healthy control subject and two USH2 patients are shown in Supplementary Figure S2. Individual fERG amplitude data plotted as a function of age are shown in Figure 1A for 47 USH2 patients (1 eye per patient; closed circles) and 62 age-matched control subjects (open diamonds, age range 12–72 years, data from 101 eyes). Lines connect longitudinal data from individual patients. The cross-sectional averages of the same data computed pooling together data in bins of 5 years (see Methods) are shown in Figure 1B. As already reported, reliable fERGs can be recorded only at the beginning of the second decade of life.[23] Examples of individual data recorded from nine patients with long-term fERG follow-up are shown in Figure 2.

fERG responses showed some short-term variability; however, a clear trend toward a progressive decline with age was evident. Intervisit variability (Supplementary Fig. S3) was within the range reported in RP.[23]

In general, fERG responses in USH2 patients were considerably lower than in age-matched healthy control subjects already at the beginning of the second decade of life. By this time, the response was within 5% of healthy control subjects in only one patient, and the average value was 40% of control values. By 25 years of age, all USH2 patients had fERGs below 0.8 uV, (i.e., 30% of control values at this age). The estimated average annual decrease in the 10 to 25 years of age range was 5%. Thus, the two main peculiar features of fERG in USH2 patients are a precocious decline with respect to normal

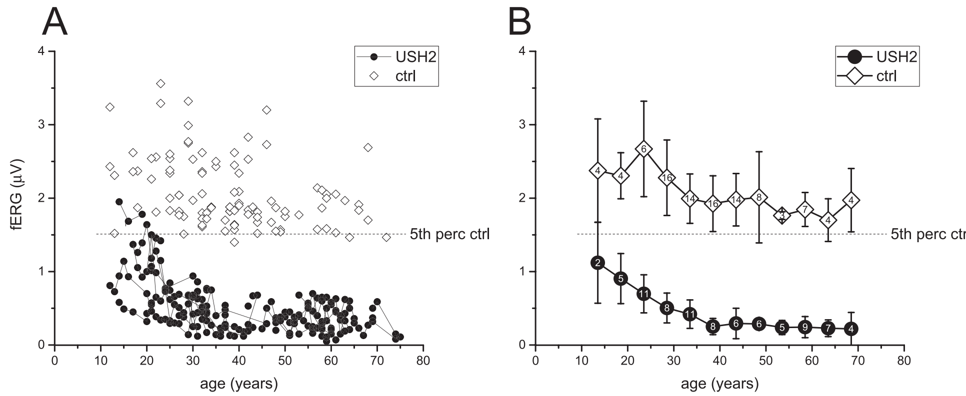

Figure 1. fERG amplitude versus age in USH2 patients and control subjects. (**A**) USH2 data (*black symbols*) are from 47 patients. Longitudinal data from individual patients are connected by lines. Control data (*open diamonds*) are from 62 subjects. The *dotted line* represent the fifth percentile of control. (**B**) Cross-sectional average of data in (**A**) averaged over 5-year age groups. Symbols as in (**A**). Numbers within the symbols indicate the number of subjects contributing to the age group average. Each patient contributes a maximum of one value (the average within the age group) to each age-group mean.

and a very narrow time window within which most of the decline occurs.

fERG Decline Compared With BCVA and Goldmann V4e Area Decline With Age

The time course of fERG amplitude decline is compared in Figure 3 with that of BCVA (plotted as logMAR) and Goldmann V4e visual field area. For each patient, the same eye is analyzed for all three measures. Dots represent individual data. Lines connect follow-up data for individual patients. fERG data for the first visit were available for 47 USH2 patients. Within this cohort, BCVA measures were available for 46 patients, and Goldmann V4e data were available for 42 patients. Follow-up data were available for 32 (fERG), 36 (BCVA), and 20 (Goldmann V4e) patients. The thick black line and the gray lines are the cross-sectional average versus age for patients and control subjects, respectively.

As already reported in previous studies,[14,15] both BCVA value and Goldmann V4e visual field are normal until at least the end of the second decade of life, both declining thereafter, with a different onset of decline from patient to patient.

Thus, the BCVA and Goldman visual field time courses are profoundly different from what observed for fERG, which is already less than half the normal values at the beginning of the second decade of life, with little further loss after 25 years of age.

These different time courses are shown in Figure 4 in terms of cross-sectional averages, expressed as percentage of control values, versus age.

This comparison further emphasizes the precocity of fERG decline and the steepness of its decline. On average, patient fERG is already down to 40% of that of control subjects by the beginning of the second decade of life, whereas BCVA cross-sectional data remain above 40% of those of control subjects, even in the sixth decade of life, and Goldman V4e cross-sectional area data go below 40% of that of controls only when patients are well into their fourth decade of life.

USH2 Patients With USH2A Identified Genetic Variants

Only a fraction of the patients analyzed in this study had undergone genotyping analysis (Table 2). When analysis was restricted only to patients with identified genetic variants, the same pattern of results as for the total patient sample was evident: a rapid and stereotyped decline of fERG with age (Supplementary Fig. S4).

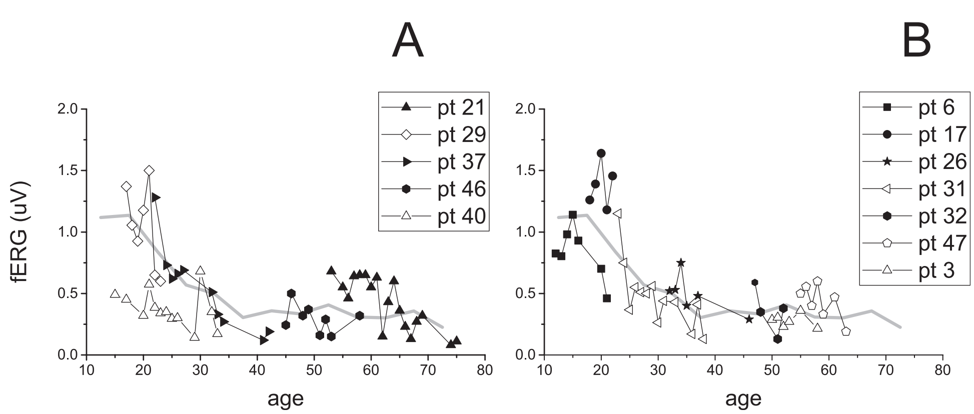

Figure 2. (**A**, **B**) Examples of individual fERG follow-up with age. In each panel, different symbols refer to different patients. The *gray lines* are the cross-sectional average over the entire patient cohort. Data are presented in two panels for clarity. Labels identify patients according to their listing in Table 1.

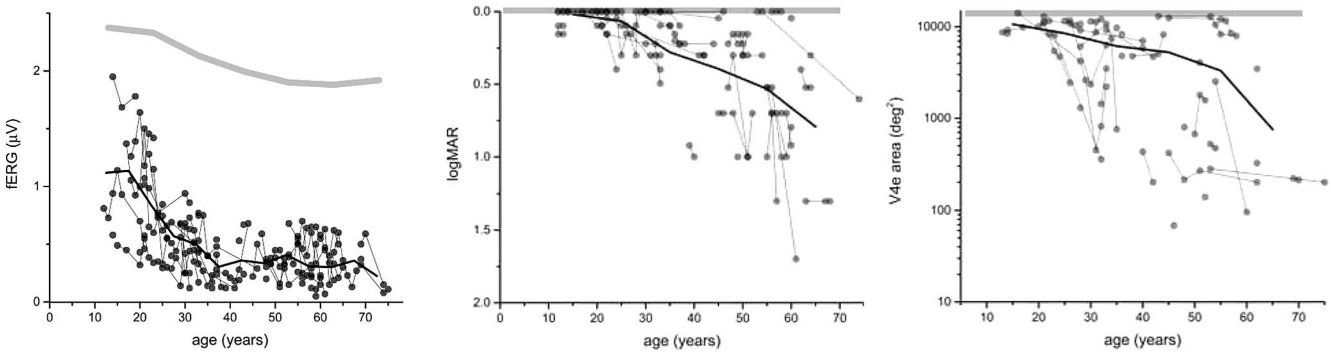

FIGURE 3. fERG, BCVA, and Goldmann V4e visual field versus age. In each plot, *gray symbols* represent individual data (longitudinal data from individual patients are connected by lines). The *thick black lines* represent the cross-sectional average versus age. The *gray horizontal lines* indicate the average values for control subjects computed over 10-year periods. fERG amplitude, logMAR, and Goldmann V4e area are presented for the same eye. fERG data are from 47 USH2 patients, of whom BCVA was available for 46 and Goldmann V4e data for 42 patients. Thirty-two patients had follow-up data for fERG, 20 for Goldmann V4e, and 36 for BCVA.

DISCUSSION

We have used fERG for more than 20 years to monitor the function of cones in the central part of normal and diseased retinas.[23–25]

The present retrospective analysis of fERG responses in USH2 patients showed that fERG amplitude is already significantly (40%) reduced with respect to control subjects at the beginning of the second decade of life, when visual acuity and Goldmann visual field are still normal. Moreover, fERG rapidly declines, reaching 25% of that of control subjects by approximately 25 years of age. A slow decline follows, soon reaching a floor level.

In other words, fERG is abnormal well in advance of other cone-related visual tests, such as visual acuity and Goldmann kinetic visual field, and most of the fERG decline is completed by 25 years of age.

Early Central Cone Deficits

These findings may have important implications for the pathophysiology of retinal dysfunction associated with USH2. Indeed, fERG data show that the central and paracentral (i.e., the 9° eccentricity from the fovea tested with fERG) cone system is compromised early in the disease process, contrary to what visual acuity would suggest.

The present results may seem at odds with the view that RP in USH is a disease that affects central cone function late in life. This view reflects the order in which a patient reports complaints about visual function, which starts from night blindness and proceed to visual field restriction and eventually visual acuity loss. Yet, central cone deficits can be detected early in life, and may represent an additional burden for patients. On a subjective basis, USH2 patients report the early need for high-contrast central stimuli to optimize vision-based performances, such as speech reading (Falsini, unpublished).

Psychophysical studies have shown abnormal foveal spectral sensitivity for short wavelengths in USH patients,[20] and abnormal foveal, focal macular, and multifocal ERGs have been reported in the early stages of RP and USH.[18,19,23,29,32,33] Furthermore, anatomic studies using adaptive optics show structural abnormalities in central cones in USH patients. Despite the presence of normal ellipsoid and interdigitation zones detectable with OCT, foveal and parafoveal cone densities were significantly reduced with respect to control data when analyzed with AOSLO.[22] These changes were mainly due to the prevalence of cones with nonwave-guiding characteristics. The abnormal cones had intact inner segments, leading to the conclusion that foveal and parafoveal cone

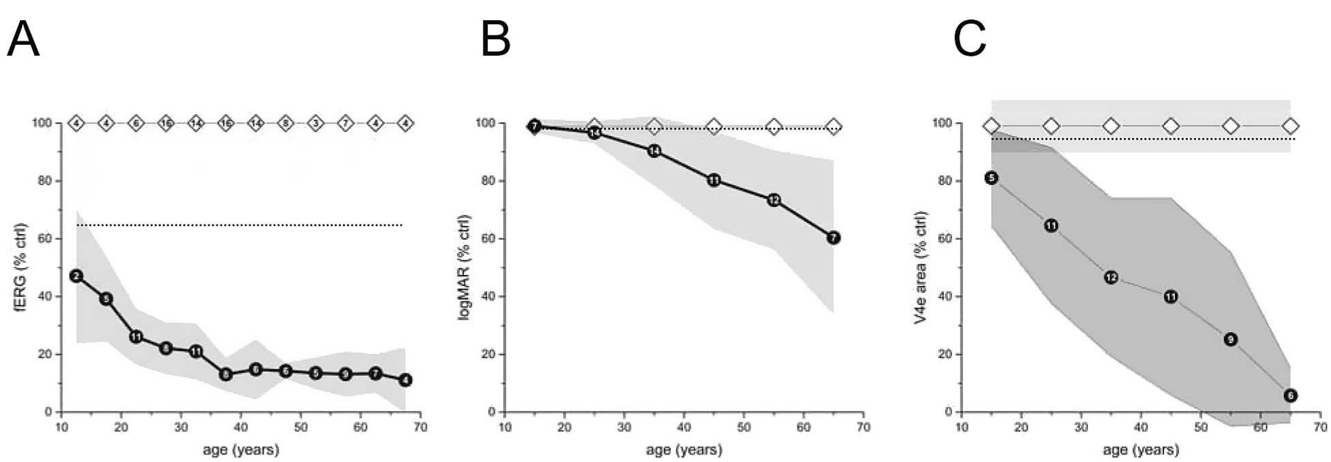

FIGURE 4. (A) fERG, (B) BCVA, (C) and Goldmann V4e visual field versus age expressed as percentage of control values. In each plot, the *black line* represents the cross-sectional average of the variable, whereas the *gray area* indicates its SD. The number within the symbols indicate the number of patients/control subjects contributing to the age-group average. The *dotted lines* represent the fifth percentile of control. For fERG and Goldman V4e, 100% is the average of control data, 0% the zero value. The logMAR range considered is from 0 (100%) to 2 (0%).

structure and density may be abnormal long before visual acuity decreases.

Indeed, cone density can be reduced by nearly 40% before visual acuity goes below 8/10 (logMAR 0.097),[22] and histopathologic studies show that RP patients may have relatively high acuity ante mortem (≥8/10), and yet retain a single rim of cones in the fovea.[34,35]

The early and rapid fERG decline we found could represent an electrophysiologic correlate of the early abnormalities in structure and density found for central cones in USH. fERG amplitude loss could reflect a reduction in the number of cone signal generators within the central 9° from which fERG response is recorded, but also a reduced quantum catching ability of the same cells, suggesting that fERG could reflect a stage of dysfunction that may precede cell loss.

Estimates of Rate of Decline in Central Cone Function Based on ERG Studies

The rate of decline of central cone function in RP patients has been evaluated in several previous studies by the use of focal or multifocal ERGs. This led to estimated average annual rates of decline ranging between a 5% and 10%. In a cohort of RP patients, Berson et al.[29] found an average annual rate of fERG amplitude decline of 5.2% using a 4°, 42-Hz stimuli. Holopigian et al.,[33] using a 9°, 40-Hz stimuli, reported an annual rate of decline of 10%. An average annual rate of decline of 6% to 10% has been found for multifocal ERG amplitudes in a cohort of RP patients including two USH patients.[32] Finally, we previously reported a 6% average annual decline for fERG (18°, 41 Hz) amplitude in 14 USH2 patients.[23]

The average annual decline of central cone function estimated on the basis of fERG in the present study is 5%, in line with previous results. The present study also shows that fERG, differently from BCVA and Goldmann visual field, decreases in a stereotyped way with age, independently of the individual age of onset of visual deficits.

fERG Decline Compared With BCVA Goldmann Visual Field Decline

In the present study, both cross-sectional and longitudinal fERG recordings indicate that central cone function is abnormal much earlier than visual acuity in USH2 patients. This indicates that assessment of central visual function should take into account that visual acuity may underestimate the abnormalities in central retinal cone function. Indeed, while we see an average annual fERG decrease of approximately 5%, and initial fERG values already down to 40% of normal at the beginning of the second decade of life, BCVA is initially normal in USH2 patients and declines at a much slower rate.

This is in line with previous studies on RP patient cohorts, showing a 2% to 3% average annual rate of decline, once BCVA begins to decrease.[33,36,37]

The finding that fERG losses precede BCVA decline by many years in USH2 patients is in accordance with a previous study on cone–rod dystrophies where we found that BCVA loss invariably followed fERG loss, with a variable delay of years.[24]

We can only speculate as to why fERG is more sensitive than BCVA to central cone deficits. fERG is an electroretinographic measure obtained as an integrated response of the whole cone system in the central 9° of the retina.[30] Conversely, BCVA is a psychophysical measure to which only the central retinal region with the highest cone density contributes. This region has been shown to be the most resistant to cone degeneration in human retinal dystrophies,[38] as well as in animal models of retinal dystrophies.[39]

The average annual rate of Goldman V4e decline in USH2 patients has been estimated to be approximately 15% to 18%,[14,15] in line with previous results in RP cohorts.[29,33,40–42] These annual rates of change are higher than what we found for fERG, but fERG starts declining much earlier than Goldmann V4e area in USH2 patients, and depends on age rather than on age of onset of visual deficits, as does Goldman perimetry decline.[15] For these reasons, fERG decline anticipates Goldmann V4e decline by many years.

One could object that the V4e isopter is not likely to be a sensitive measure of change in central cone function. However, the Goldman III4e isopter, which probably more accurately reflects central cone function than the V4e isopter, did not show any correlation with fERG (data not shown). A possible explanation for this lack of correlation is that fERG is a direct measure of retinal function, whereas Goldman visual field measures require subjective responses, and thus also involve post retinal processing.

fERG Limitations

Like all techniques, fERG has limitations. In particular, fERG provides information about losses in the central macular region; but, unlike multifocal ERG, it does not provide topographic information. In addition, as we showed here, its precocious decline makes it most useful in an early age window, whereas, with disease progression, other measures, such as static perimetry, autofluorescence, and/or analysis of the extent of the intact ellipsoid zone band as a marker of usable visual field, may be more useful to follow disease progression.

Clinical Implications

In the present study, we found no apparent relationship between fERG decline and either BCVA or Goldman V4e decline. Indeed, whereas the onset of BCVA and Goldmann field decay varies from patient to patient,[14,15,36] fERG decline occurs in a restricted age window, with 75% of the loss occurring by 25 years of age in all patients.

In this respect, BCVA and Goldmann measurements appear more valuable than fERG for patients, because with these measures clinicians can provide indications of rates of decline to the patient, once the disease has established its course.[14–16,31,36,43]

Conversely, fERG decline does not seem to depend on disease onset, but rather it follows an almost stereotyped course with age. It can still be used to estimate the average rate of central cone function decay,[23] but its restricted and almost invariant age window of decline makes it most of all a hallmark of the disease. Yet, finding an indicator of early central cone dysfunction may have important implications for any attempt toward therapeutic approaches, being for instance a possible early readout of the intervention efficacy.

In conclusion, this study shows the usefulness of fERG to monitor central cone decline in USH2 patients, particularly in the early stages of the disease. This is in line with a number of previously published studies showing the usefulness of focal ERG and multifocal ERG in detecting central visual deficits in RP patients.

Acknowledgments

The authors thank Nicoletta Berardi and Alessandro Sale for critical reading of the manuscript.

Supported by grants from Rare Partners onlus (BF; Milan, Italy), ex 60% MIUR (BF; Rome, Italy), and Fondazione Roma (LGR; Rome, Italy).

Disclosure: **L. Galli-Resta**, None; **G. Placidi**, None; **F. Campagna**, None; **L. Ziccardi**, None; **M. Piccardi**, None; **A. Minnella**, None; **E. Abed**, None; **S. Iovine**, None; **P. Maltese**, None; **M. Bertelli**, None; **B. Falsini**, None

References

1. Fishman GA, Kumar A, Joseph ME, Torok N, Anderson RJ. Usher's syndrome. Ophthalmic and neuro-otologic findings suggesting genetic heterogeneity. *Arch Ophthalmol*. 1983;101:1367–1374.
2. Keats BJ, Corey DP. The usher syndromes. *Am J Med Genet*. 1999;89:158–166.
3. Mets MB, Young NM, Pass A, Lasky JB. Early diagnosis of Usher syndrome in children. *Trans Am Ophthalmol Soc*. 2000;98: 237–242; discussion 243–245.
4. Loundon N, Marlin S, Busquet D, et al. Usher syndrome and cochlear implantation. *Otol Neurotol*. 2003;24:216–221.
5. Kimberling WJ, Hildebrand MS, Shearer AE, et al. Frequency of Usher syndrome in two pediatric populations: implications for genetic screening of deaf and hard of hearing children. *Genet Med*. 2010;12:512–516.
6. Petit C. Usher syndrome: from genetics to pathogenesis. *Annu Rev Genomics Hum Genet*. 2001;2:271–297.
7. Boughman JA, Vernon M, Shaver KA. Usher syndrome: definition and estimate of prevalence from two high-risk populations. *J Chronic Dis*. 1983;36:595–603.
8. Davenport SLH, Omenn GS. The heterogeneity of Usher syndrome. In: Littlefield JW, de Grouchy J, Ebling FJG. Proceedings of the 5th International Conference on Birth Defects, Montreal, Canada, 21-27 August, 1997. Amsterdam: Excerpta Medica; 1977.
9. Smith RJ, Berlin CI, Hejtmancik JF, et al. Clinical diagnosis of the Usher syndromes. Usher Syndrome Consortium. *Am J Med Genet*. 1994;50:32–38.
10. Grondahl J. Estimation of prognosis and prevalence of retinitis pigmentosa and Usher syndrome in Norway. *Clin Genet*. 1987;31:255–264.
11. Hope CI, Bundey S, Proops D, Fielder AR. Usher syndrome in the city of Birmingham–prevalence and clinical classification. *Br J Ophthalmol*. 1997;81:46–53.
12. Rosenberg T, Haim M, Hauch AM, Parving A. The prevalence of Usher syndrome and other retinal dystrophy-hearing impairment associations. *Clin Genet*. 1997;51:314–321.
13. Spandau UH, Rohrschneider K. Prevalence and geographical distribution of Usher syndrome in Germany. *Graefes Arch Clin Exp Ophthalmol*. 2002;240:495–498.
14. Fishman GA, Bozbeyoglu S, Massof RW, Kimberling W. Natural course of visual field loss in patients with Type 2 Usher syndrome. *Retina*. 2007;27:601–608.
15. Iannaccone A, Kritchevsky SB, Ciccarelli ML, et al. Kinetics of visual field loss in Usher syndrome Type II. *Invest Ophthalmol Vis Sci*. 2004;45:784–792.
16. Edwards A, Fishman GA, Anderson RJ, Grover S, Derlacki DJ. Visual acuity and visual field impairment in Usher syndrome. *Arch Ophthalmol*. 1998;116:165–168.
17. van Meel GJ, van Norren D. Foveal densitometry in retinitis pigmentosa. *Invest Ophthalmol Vis Sci*. 1983;24:1123–1130.
18. Biersdorf WR. The clinical utility of the foveal electroretinogram: a review. *Doc Ophthalmol*. 1989;73:313–325.
19. Iarossi G, Falsini B, Piccardi M. Regional cone dysfunction in retinitis pigmentosa evaluated by flicker ERGs: relationship with perimetric sensitivity losses. *Invest Ophthalmol Vis Sci*. 2003;44:866–874.
20. Alexander KR, Hutman LP, Fishman GA. Dark-adapted foveal thresholds and visual acuity in retinitis pigmentosa. *Arch Ophthalmol*. 1986;104:390–394.
21. Sumaroka A, Matsui R, Cideciyan AV, et al. Outer retinal changes including the ellipsoid zone band in Usher syndrome 1B due to MYO7A mutations. *Invest Ophthalmol Vis Sci*. 2016;57:OCT253–OCT261.
22. Sun LW, Johnson RD, Langlo CS, et al. Assessing photoreceptor structure in retinitis pigmentosa and Usher syndrome. *Invest Ophthalmol Vis Sci* 2016;57:2428–2442.
23. Falsini B, Galli-Resta L, Fadda A, et al. Long-term decline of central cone function in retinitis pigmentosa evaluated by focal electroretinogram. *Invest Ophthalmol Vis Sci*. 2012;53: 7701–7709.
24. Galli-Resta L, Piccardi M, Ziccardi L, et al. Early detection of central visual function decline in cone-rod dystrophy by the use of macular focal cone electroretinogram. *Invest Ophthalmol Vis Sci*. 2013;54:6560–6569.
25. Galli-Resta L, Falsini B, Rossi G, et al. Bilateral symmetry of visual function loss in cone-rod dystrophies. *Invest Ophthalmol Vis Sci*. 2016;57:3759–3768.
26. Kumar A, Fishman G, Torok N. Vestibular and auditory function in Usher's syndrome. *Ann Otol Rhinol Laryngol*. 1984;93:600–608.
27. Bonnet C, Riahi Z, Chantot-Bastaraud S, et al. An innovative strategy for the molecular diagnosis of Usher syndrome identifies causal biallelic mutations in 93% of European patients. *Eur J Hum Genet*. 2016;24:1730–1738.
28. Maltese PE, Orlova N, Krasikova E, et al. Gene-targeted analysis of clinically diagnosed long QT Russian families. *Int Heart J*. 2017;58:81–87.
29. Berson EL, Sandberg MA, Rosner B, Birch DG, Hanson AH. Natural course of retinitis pigmentosa over a three-year interval. *Am J Ophthalmol*. 1985;99:240–251.
30. Falsini B, Iarossi G, Fadda A, et al. The fundamental and second harmonic of the photopic flicker electroretinogram: temporal frequency-dependent abnormalities in retinitis pigmentosa. *Clin Neurophysiol*. 1999;110:1554–1562.
31. Testa F, Melillo P, Bonnet C, et al. Clinical presentation and disease course of Usher Syndrome because of mutations in Myo7a or Ush2a. *Retina*. 2017;37:1581–1590.
32. Nagy D, Schonfisch B, Zrenner E, Jagle H. Long-term follow-up of retinitis pigmentosa patients with multifocal electroretinography. *Invest Ophthalmol Vis Sci*. 2008;49:4664–4671.
33. Holopigian K, Greenstein V, Seiple W, Carr RE. Rates of change differ among measures of visual function in patients with retinitis pigmentosa. *Ophthalmology*. 1996;103:398–405.
34. Kolb H, Gouras P. Electron microscopic observations of human retinitis pigmentosa, dominantly inherited. *Invest Ophthalmol*. 1974;13:487–498.
35. Milam AH, Li ZY, Fariss RN. Histopathology of the human retina in retinitis pigmentosa. *Prog Retin Eye Res*. 1998;17: 175–205.
36. Sandberg MA, Rosner B, Weigel-DiFranco C, et al. Disease course in patients with autosomal recessive retinitis pigmentosa due to the USH2A gene. *Invest Ophthalmol Vis Sci*. 2008; 49:5532–5539.
37. Birch DG, Anderson JL, Fish GE. Yearly rates of rod and cone functional loss in retinitis pigmentosa and cone-rod dystrophy. *Ophthalmology*. 1999;106:258–268.
38. Jacobson SG, Roman AJ, Aleman TS, et al. Normal central retinal function and structure preserved in retinitis pigmentosa. *Invest Ophthalmol Vis Sci*. 2010;51:1079–1085.
39. Punzo C, Xiong W, Cepko CL. Loss of daylight vision in retinal degeneration: are oxidative stress and metabolic dysregulation to blame? *J Biol Chem*. 2012;287:1642–1648.

40. Madreperla SA, Palmer RW, Massof RW, Finkelstein D. Visual acuity loss in retinitis pigmentosa. Relationship to visual field loss. *Arch Ophthalmol* 1990;108:358–361.

41. Grover S, Fishman GA, Anderson RJ, Lindeman M. A longitudinal study of visual function in carriers of X-linked recessive retinitis pigmentosa. *Ophthalmology*. 2000;107: 386–396.

42. Massof RW, Dagnelie G, Benzschawel T, Palmer RW, Finkelstein D. First-order dynamics of visual field loss in retinitis pigmentosa. *Clin Vis Sci*. 1990;5:1–26.

43. Piazza L, Fishman GA, Farber M, Derlacki D, Anderson RJ. Visual acuity loss in patients with Usher's syndrome. *Arch Ophthalmol*. 1986;104:1336–1339.

44. Richards S, Aziz N, Bale S, et al; for the ACMG Laboratory Quality Assurance Committee. Standards and guidelines for the interpretation of sequence variants: a joint consensus recommendation of the American College of Medical Genetics and Genomics and the Association for Molecular Pathology. *Genet Med*. 2015;17:405–424.